Synthesis, biological evaluation and structure–activity correlation study of a series of imidazol-based compounds as Candida albicans inhibitors

ARTICLE *in* EUROPEAN JOURNAL OF MEDICINAL CHEMISTRY · JULY 2014

Impact Factor: 3.45 · DOI: 10.1016/j.ejmech.2014.07.001 · Source: PubMed

12 AUTHORS, INCLUDING:

Roberto Di Santo
Sapienza University of Rome
129 PUBLICATIONS **1,755** CITATIONS
SEE PROFILE

Roberta Costi
Sapienza University of Rome
101 PUBLICATIONS **1,451** CITATIONS
SEE PROFILE

Roberto Cirilli
Istituto Superiore di Sanità
99 PUBLICATIONS **1,415** CITATIONS
SEE PROFILE

Giovanna Simonetti
Sapienza University of Rome
51 PUBLICATIONS **390** CITATIONS
SEE PROFILE

European Journal of Medicinal Chemistry 83 (2014) 665–673

Contents lists available at ScienceDirect

European Journal of Medicinal Chemistry

journal homepage: http://www.elsevier.com/locate/ejmech

Original article

Synthesis, biological evaluation and structure–activity correlation study of a series of imidazol-based compounds as *Candida albicans* inhibitors

Francesca Moraca [d, 1], Daniela De Vita [a, 1], Fabiana Pandolfi [a], Roberto Di Santo [a, b], Roberta Costi [a, b], Roberto Cirilli [e], Felicia Diodata D'Auria [c], Simona Panella [c], Anna Teresa Palamara [c], Giovanna Simonetti [c], Maurizio Botta [d, **], Luigi Scipione [a, *]

[a] Department of "Chimica e Tecnologie del Farmaco", Sapienza University of Rome, Piazzale Aldo Moro, 5, 00185 Rome, Italy
[b] "Istituto Pasteur-Fondazione Cenci Bolognetti", Department of "Chimica e Tecnologie del Farmaco", Sapienza University of Rome, Piazzale Aldo Moro, 5, 00185 Rome, Italy
[c] Department of "Sanità Pubblica e Malattie Infettive", Sapienza University of Rome, Piazzale Aldo Moro, 5, 00185 Rome, Italy
[d] Department of "Biotecnologie, Chimica e Farmacia", "Università degli Studi di Siena", Via A. Moro 2, 53100 Siena, Italy
[e] "Dipartimento del Farmaco", Istituto Superiore di Sanità, Viale Regina Elena 299, 00161 Rome, Italy

ARTICLE INFO

Article history:
Received 25 April 2014
Received in revised form
25 June 2014
Accepted 1 July 2014
Available online 1 July 2014

Keywords:
Antifungal
Azole derivatives
Enantioselective synthesis
Ligand-based drug design

ABSTRACT

A new series of 2-(1H-imidazol-1-yl)-1-phenylethanol derivatives was synthesized. The antifungal activity was evaluated *in vitro* against different fungal species. The biological results show that the most active compounds possess an antifungal activity comparable or higher than Fluconazole against *Candida albicans*, non-albicans *Candida* species, *Cryptococcus neoformans* and dermathophytes. Because of their racemic nature, the most active compounds **5f** and **6c** were tested as pure enantiomers. For **6c** the (*R*)-enantiomer resulted more active than the (*S*)-one, otherwise for **5f** the (*S*)-enantiomer resulted the most active. To rationalize the experimental data, a ligand-based computational study was carried out; the results of the modelling study show that (*S*)-**5f** and (*R*)-**6c** perfectly align to the ligand-based model, showing the same relative configuration. Preliminary studies on the human lung adenocarcinoma epithelial cells (A549) have shown that **6c**, **5e** and **5f** possess a low cytotoxicity.

1. Introduction

Fungi infect billions of people every year and millions contract diseases that kill at least as many people as tuberculosis or malaria [1]. The highly fatal fungal systemic infections are supported mainly by *Candida albicans*, *Candida* species non *albicans*, *Cryptococcus neoformans* and *Aspergillus* spp. Superficial mucosal and cutaneous infections are mainly supported by *Candida* spp. and dermatophytes.

Despite the antifungal drugs used in clinical treatments appear to be diverse and numerous, to date few classes of antifungal agents are currently available to treat mucosal or systemic infections [2]. The largest family of antifungal drugs is represented by the azole compounds i.e. imidazoles (Miconazole, Econazole, Clotrimazole, and Ketoconazole) and triazoles (Fluconazole, Itraconazole, and the latest agents, Voriconazole and Posaconazole) (Chart 1) [3–5]. Azoles block fungal membrane ergosterol biosynthesis in the cell by inhibiting the activity of the lanosterol 14α-demethylase, the enzyme necessary to convert lanosterol to ergosterol. The active binding site of lanosterol demethylase contains a heme domain. Azoles bind with a nitrogen atom to the iron atom of the heme, preventing the demethylation of lanosterol [6]. The depletion of ergosterol and accumulation of 14α-methylated sterols disrupt the structure and many functions of fungal membrane leading to inhibition of fungal growth [7].

However, the treatment of invasive fungal diseases still remains unsatisfied as mortality rate, is unacceptable high [8]. Moreover, non-invasive infections, as onychomycoses, are often recurrent, chronic, and generally require long-term treatment with antifungal agents [9]. Hence, there is considerable urgency to discover new antimicrobial agents.

* Corresponding author.
** Corresponding author.
E-mail addresses: maurizio.botta@unisi.it (M. Botta), Luigi.scipione@uniroma1.it, luigi.scipione@fastwebnet.it (L. Scipione).
[1] These authors equally contribute to the work.

http://dx.doi.org/10.1016/j.ejmech.2014.07.001
0223-5234/

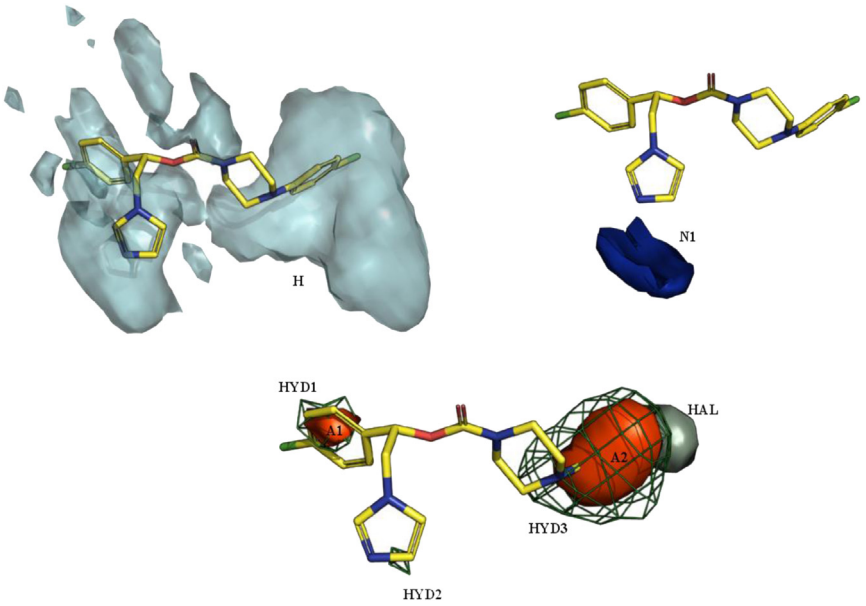

Fig. 1. Contour maps of the ligand-based model generated according to GRID MIFs. A: Cyan surface represents the shape that active compounds should match; B: N1 = blue lone pair nitrogen counter maps; C: HAL1 = grey halogen counter map; A–A2 = orange aromatic counter maps; HYD1–HYD3 = blue marine mesh hydrophobic counter maps. In yellow sticks is represented compound (*S*)-**5f**. (For interpretation of the references to colour in this figure legend, the reader is referred to the web version of this article.)

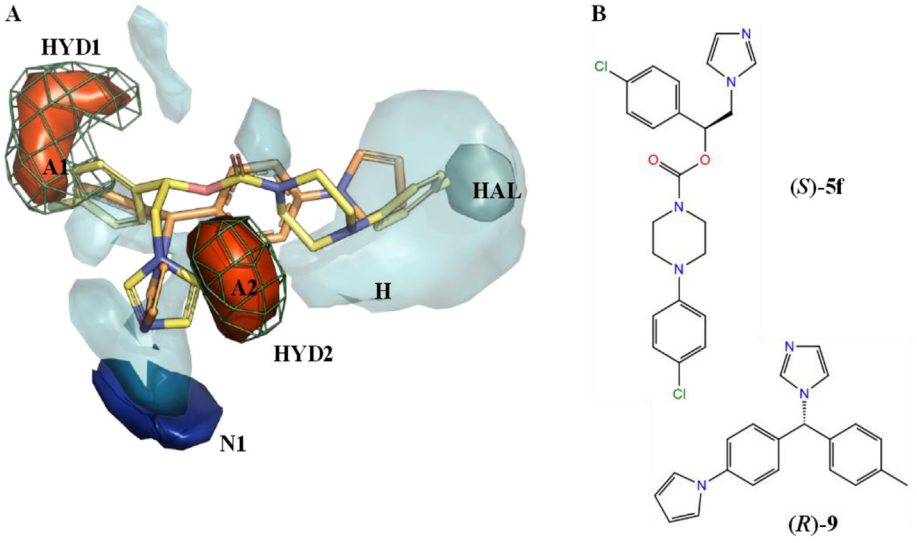

Fig. 2. A; contour maps of the LBM2 model are the same as described in Fig. 1. In yellow stick is represented compound (*S*)-**5f** and in orange stick compound (*R*)-**9**. Non-polar hydrogen atoms are omitted. B; structure of the most active compounds (*S*)-**5f** and (*R*)-**9**. (For interpretation of the references to colour in this figure legend, the reader is referred to the web version of this article.)

We have previously reported the synthesis and *in vitro* evaluation of antifungal activity of a new series of 2-(1H-imidazol-1-yl)-1-phenylethanol derivatives [10]. Given the azole nature of those compounds, we hypothesized CYP51 as the target and focused on the design and synthesis of new imidazole derivatives, modifying the side chain of 2-(1H-imidazol-1yl)-ethyl carbamates or esters previously reported, in order to improve their antifungal activity [10]. All the new synthetized compounds were tested *in vitro* to evaluate the antifungal activity against different fungal strains and some of them showed high inhibitory activity. Up to date, there is no three dimensional structural information available on *C. albicans* (CACYP51) or other fungal CYP51 enzymes. Therefore, computational techniques were used to rationalize the experimental data. A ligand-based approach helped the discrimination between active and inactive compounds in fully agreement with the *in vitro* data, giving useful information about the functional groups that could be responsible for the antifungal activity.

2. Results and discussion

2.1. Chemistry

The racemic 2-(1*H*-imidazol-1-yl)-1-phenylethanols **1a**–**c**, the esters **2a**,**b** and **3a**–**g** and the carbamates **4a**–**c** were prepared as

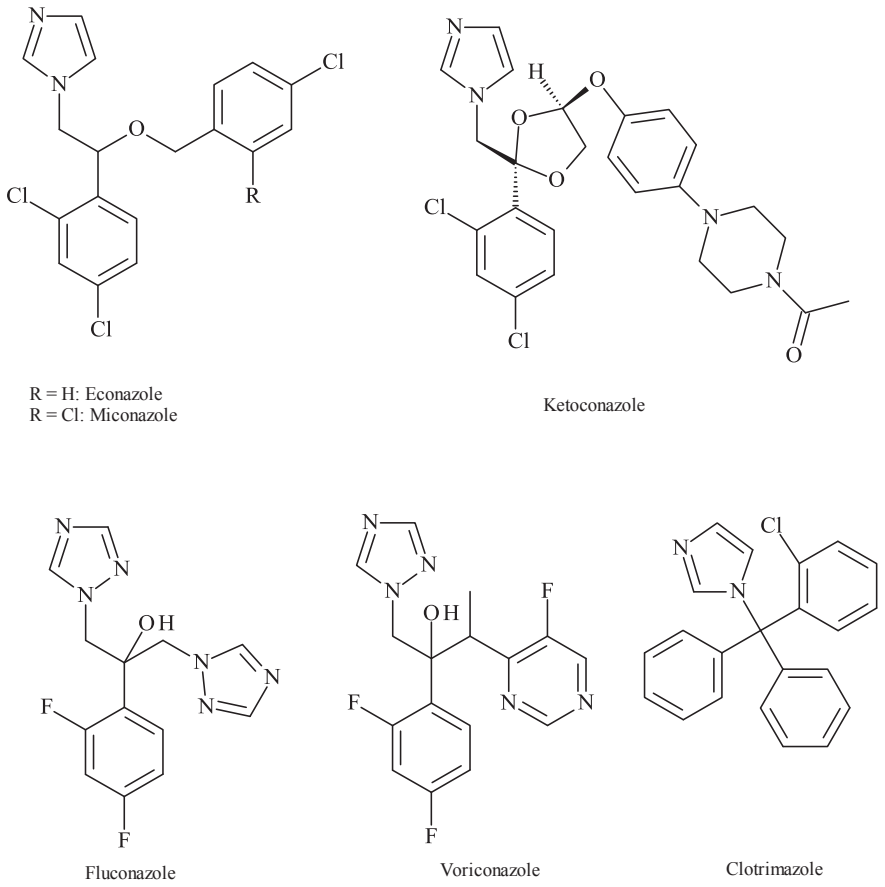

Chart 1. Main azole drugs used for the treatment of candidiasis.

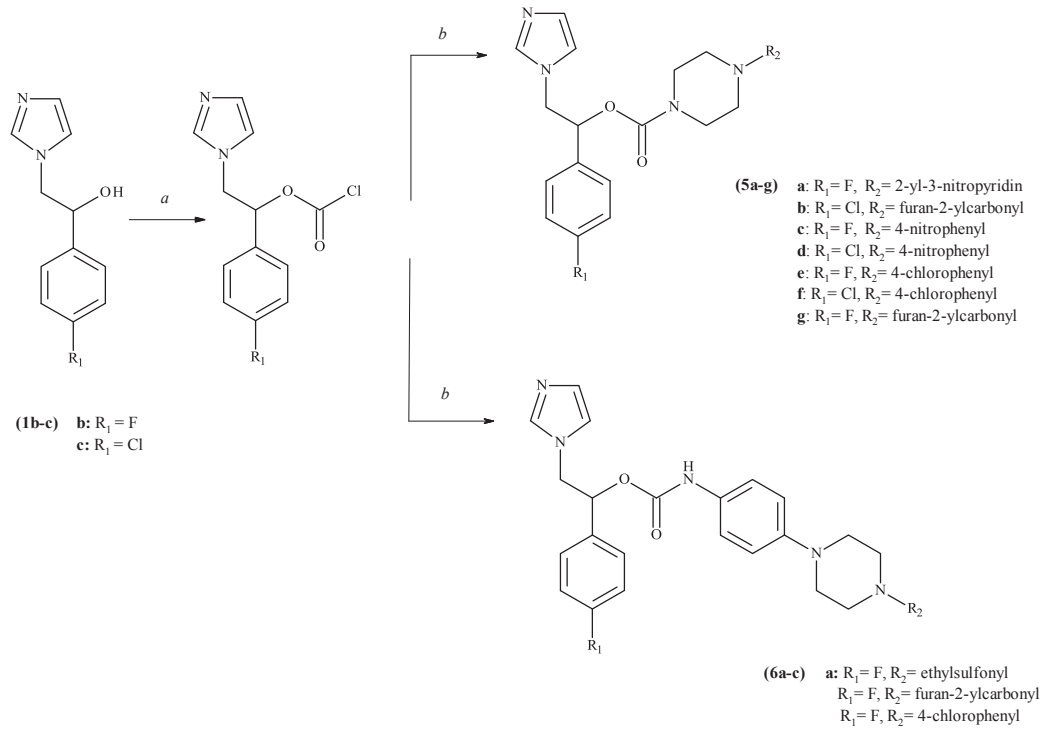

Scheme 1. Preparation of compounds **5a**–**g** and **6a**–**c**. Reagents and conditions: (*a*) dry CH_3CN, triphosgene, rt, overnight; (*b*) TEA, selected amine, rt, overnight.

described in the literature [10]. The pure enantiomers of **1b,c** have been prepared using the procedure described in our previous letter [11]. The synthesis of **5a–g** and **6a–c** was carried out using triphosgene in dry CH_3CN to obtain activation of the –OH group as chloroformate of the appropriate 2-(1*H*-imidazol-1-yl)-1-phenylethanol; then the mixture was added with TEA and the selected amine and stirred overnight as described in Scheme 1. Commercial available amines have been used to synthesize the compounds **5b–g**. The side chains for the synthesis of **5a** is prepared as reported in Scheme 2, by condensation of the piperazine with 2-chloro-3-nitropyridine. The required amines for the synthesis of the side chains of compounds **6a–c** were prepared as described in Scheme 3. The synthesis was carried out by condensation of 1-fluoro-4-nitrobenzene with the appropriate commercial piperazine in CH_3CN under reflux condition for 2 h. Then the nitro group was converted to amino group by reduction with H_2–Pd/C. The obtained amines were used immediately.

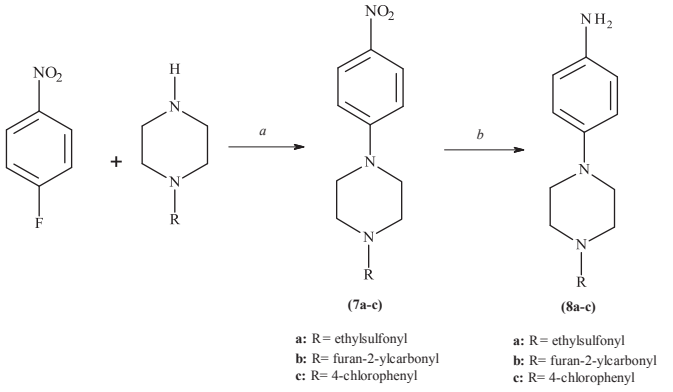

Scheme 3. Preparation of the side chains of **6a–c**. Reagents and conditions: (*a*) CH_3CN, reflux, 2 h; (*b*) H_2, Pd/C, 50 psi, 4 h, rt.

2.2. In vitro antifungal activity and cytotoxicity

The antifungal activity of the synthesized compounds was evaluated by CLSI broth microdilution methods against different strains of *C. albicans*, non-albicans *Candida* species, *C. neoformans* and dermathophytes. Fluconazole (Flu) was used as reference drug.

The antifungal activity was expressed as MIC_{50} (μg mL^{-1}) for the yeasts (the lowest concentration that showed ≥50% growth inhibition compared with the control) and as MIC_{80} (μg mL^{-1}) for the dermatophytes (the lowest concentration that showed ≥80% growth inhibition compared with the control). For each fungal strain the results were reported as the median of the MIC values of five replicates and for all the strains within to *C. albicans*, non-albicans *Candida* species, *C. neoformans* and dermatophytes the geometric mean (GM) value was reported in Table 1.

The data in Table 1 show that the compounds **5e**, **5f** and **6c** possess an interesting antifungal activity. In particular, we found that **5e** and **6c** show GM MIC values of 1.87 and 1.81 μg mL^{-1}, against *C. albicans*, comparable to Flu, otherwise **5f** shows a GM MIC value of 0.67 μg mL^{-1} resulting more active than Flu. Furthermore, **5e**, **5f** and **6c** also resulted more active than Flu against non-albicans *Candida* species with GM MIC values respectively of 2.06, 1.83 and 0.51 μg mL^{-1}. Compound **6c** also resulted more active than Flu towards *C. neoformans* (GM MIC 0.22 μg mL^{-1}) and towards dermathophytes (GM MIC 6.35 μg mL^{-1}). Moreover, compound **5f** show a GM MIC value of 3.70 μg mL^{-1} against dermathophytes and resulted more potent than Flu.

In the Tables S1–S4 of the supplementary information the detailed results obtained for each strain of *C. albicans*, non-albicans *Candida* species, *C. neoformans* and dermathophytes are reported.

Because of their racemic nature, the most active compounds **5f** and **6c** were tested as pure (*R*)- and (*S*)-enantiomers to evaluate if they possess a different antifungal activity. (*R*)-**6c** resulted more active than Flu against *C. albicans*, non-albicans *Candida* species, *C. neoformans*, and dermathophytes with GM MIC values

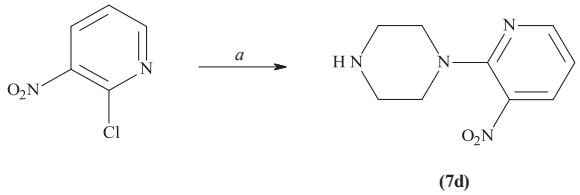

(7d)

Scheme 2. Preparation of side chain of **5a** (**7d**). Reagents and conditions: (*a*) CH_3CN, piperazine dihydrochloride hydrate, TEA, reflux, 2 h.

respectively of 0.20, 0.25, 0.17 and 3.17 μg mL^{-1}. Moreover, (*S*)-**5f** was found more active than Flu against *C. albicans*, non-albicans *Candida* species and dermathophytes with GM MIC values respectively of 0.27, 1.33 and 3.61 μg mL^{-1}.

The antifungal activity of **5f**, (*S*)-**5f**, **6c** and (*R*)-**6c**, was also evaluated towards some Fluconazole resistant *Candida* species and the activity was reported as geometric mean of MIC (GM-MIC μg mL^{-1}) in Table 1. The obtained results indicate that all the new compounds were more active than Flu on the resistant fungal strains; particularly (*R*)-**6c** showed a GM MIC value of 2.97 μg mL^{-1} and (*S*)-**5f** a GM MIC value 4.56 μg mL^{-1}, resulting about fifteen and tenfold more active than Flu (GM MIC 44.51 μg mL^{-1}).

Preliminary studies carried out on **5e**, **5f** and **6c**, have shown that the above compounds possess a low cytotoxicity on the human lung adenocarcinoma epithelial cells (A549) with CC_{50} values respectively of 78.4, 82.2 and 171.8 μg mL^{-1} (Table 2).

2.3. Structure–activity correlation based on GRID MIFs

Given the structural similarity of the compounds presented here to known antifungal CYP51 inhibitors, this enzyme has been proposed as the target. However, there are no three dimensional structural information about *C. albicans* CYP51, hence it has been developed a ligand-based structure–activity correlation study by means of GRID MIFs (Molecular Interaction Fields) on the 27 azole-based compounds (Chart 2), some of which previously reported [10], evaluated *in vitro* against *C. albicans* (Table S6 supporting info), in order to help the rationalization of experimental data. The ligand-based model is able to help the discrimination between active and inactive compounds, in fully agreement with the *in vitro* data, giving useful insights for the understanding of the functional groups possibly responsible for the antifungal activity. In a previous work [12] we reported a pharmacophore hypothesis (HYPO1) derived from a 3D-QSAR study on 1-[(aryl)[4-aryl-1H-pyrrol-3-yl]-1H-imidazole as *C. albicans* CYP51 inhibitors, described elsewhere [12]. The HYPO1 showed an aromatic feature with a lone pair nitrogen in the ring plane and three aromatic features. According to HYPO1, an ideal CYP51 inhibitor should show (i) an aromatic nitrogen with an accessible lone pair; (ii) a diarylmethyl moiety on the azole N-1, which is preferred over a 1,2-diarylethyl; (iii) one of the two aryls on the methyl group could be better a phenyl ring with a para lypophilic substituent; (iv) the second aryl group should be made up of two coplanar aromatic rings. Qualitatively, our ligand-based model (thereafter called LBM) shows similarities to the previously reported HYPO1, supporting our hypothesis of CYP51 as the target enzyme of the azole-based compounds

Table 1
In vitro antifungal activity of studied compounds against *Candida albicans*, *Candida* species, *Cryptococcus neoformans* and dermathophytes.

Cmp	*C. albicans*[a] GM MIC (μg mL^{-1})	*Candida* species[b] GM MIC (μg mL^{-1})	*C. neoformans*[c] GM MIC (μg mL^{-1})	Dermathophytes[d] GM MIC (μg mL^{-1})	*Candida* species resistant strains[e] GM MIC (μg mL^{-1})
5a	11.31	11.99	4.49	27.43	nd
5b	58.69	128.00	90.51	128	nd
5c	17.75	32.00	21.98	50.79	nd
5d	13.22	34.90	12.34	34.56	nd
5e	1.87	2.06	3.00	13.03	nd
5f	0.67	1.83	3.17	3.7	7.25
(*R*)-**5f**	5.86	15.54	3.36	7.03	nd
(*S*)-**5f**	0.27	1.33	2.52	3.61	4.56
5g	85.92	50.80	98.70	109.73	nd
6a	128.00	128.00	16.95	128	nd
6b	111.43	128.00	16.00	118.51	nd
6c	1.81	0.51	0.22	6.35	5.38
(*R*)-**6c**	0.20	0.25	0.17	3.17	2.97
(*S*)-**6c**	40.09	3.89	1.41	118.51	nd
Flu	1.27	2.91	1.89	7.2	44.51

Data represent the geometric mean of minimal inhibitory concentration (GM MIC) of five replicates.
[a] *C. albicans* strains: ATCC24433, ATCC3153, ATCC10231, ATCC76615, ATCC10261, ATCC90028, ATCC20891, PMC1011.
[b] *Candida* species strains: *C. krusei* DSM6128 and PMC0613, *C. tropicalis* PMC0910 and DSM11953, *C. parapsilosis* DSM11224 and ATCC22019, *C. glabrata* PMC0805 and PMC0807.
[c] *C. neoformans* strains: PMC2123, PMC2136, PMC2115, PMC2103, PMC2107, PMC2102, DSM11959, PMC2111.
[d] Dermathophytes strains: *T. mentagrophytes* DSM4870, PMC6515, PMC6531, PMC6509, PMC6503 and PMC6552, *M. gypseum* PMC7303, PMC7331 and DSM3824.
[e] *Candida* species resistant strains: *C .albicans* PMC1040R, PMC1041R and PMC1042R, *C. glabrata* PMC0850R, PMC0851R, PMC0852R and PMC0853R; nd: not determined.

reported in this paper. As in HYPO1, LBM shows a blue contour map representing a region that leads to the enhancement of activity with a lone pair nitrogen, possibly able to interact with the iron atom of the heme prosthetic group; two orange contour maps and two green contour maps that are representative of favourable regions for aromatic and hydrophobic groups respectively. The differences to the previous HYPO1 are the presence of a grey contour map that represents a region favourable for halogen substituents and a cyan contour map that represents the shape that an active compound should match (Fig. 1).

The active azole-based compounds presented show most of their functional groups within the above described contour maps, that can explain the reason of their higher activity. It is worth noting the highest activity of compound (*R*)-**5f** with respect to its −*S* enantiomer and the other active compounds. The reason of the decrease of their activity with respect to the most active (*S*)-**5f** is not evident from the ligand-based model but, assuming CYP51 as the target enzyme, it is possible that those compounds show a worst coordination at the heme iron with respect to (*R*)-**5f**. To show a good coordination at the heme prosthetic group, a compound should place its heme-coordinating group perpendicularly to the heme iron, as reported by Holtje et al. and subsequently by us [11,13]. After the alignment of compounds, it is evident that the imidazolic ring of the less active (*R*)-**5f** has a slightly different orientation with respect to the imidazolic ring of the other active compounds, that could support this hypothesis. All the active compounds show the alignment to the A1 and HYD1 contour maps, highlighting the importance of non-polar interactions in this region. Compound (*S*)-**6c** that does not align to LBM, is much less active than−*R* enantiomer. In addition, it is evident from our data that compounds possessing a fluorine atom in correspondence to the HAL contour map are less active than compounds that show a chlorine substituent. Compounds **3e**, **3g** and **3f**, are the only actives that do not show a halogen substituent alignment to the HAL contour map, but are the only that show two phenyl rings directly linked together (as in the antifungal bifonazole) that in LBM are aligned to the HYD3 contour map, emphasizing the importance of non-polar interactions in this region. This is another useful information to understand the difference in the activity of compounds that show a similar scaffold. All the inactive compounds lose functional groups aligned to the A1 and HYD1 contour maps and to the HAL contour map, emphasizing the importance of the presence of halogens in this region and/or the presence of more hydrophobic moieties aligned to the HYD3 contour map. The inactive compounds **1a**, **1b** and **1c** represent a fragment of the most active compound (*S*)-**5f**, hence a good starting point for the synthesis of more potent compounds, on the basis of the study reported here. To give more value to this study and to propose a general SAR for the further design of highly potent antifungal agents, we built a second ligand-based model (LBM2) combining information taken from this study and the already reported one [12]. Hence, LBM2 derives from the alignment of the antifungal drugs bifonazole, miconazole, fluconazole, our most active compounds (*S*)-**5f** and the most active compounds (*R*)-**9** taken from the previous study [12]. LBM2 summarizes the essential characteristics that an active compound towards *C. albicans* CYP51 should possess. It shows i) a lone pair nitrogen contour map, of pivotal importance for the interaction with the heme iron of the prosthetic group; ii) two aromatic and two hydrophobic contour maps, of which A1 and HYD1 correspond to an aromatic or an aliphatic ring that enhance hydrophobic interactions in this region, A2 and HYD2 to the imidazolic ring coordinating the heme iron; iii) a halogen contour map and a characteristic shape (Fig. 2). LBM2 is also in agreement with the refined pharmacophoric model proposed by Di Santo et al. (2005) (MOD3) [14]. Indeed, MOD3 shows i) a feature for unsubstituted aromatic nitrogen; ii) a feature for aromatic rings; iii) two features for hydrophobic moieties. In addition, it shows two excluded volumes indicating the portion of space that an active compound should not match, slightly recalling the shape proposed by our LBM2 model.

3. Conclusion

The biological *in vitro* data show that some of the synthesized compounds possess an interesting antifungal activity versus *Candida* species and other fungal species. The structural modifications of the side chain allowed us to obtain some new compounds with high antifungal activity. In particular **5e**, **5f** and **6c** showed activity similar to or higher than Flu against *C. albicans* and *Candida* species, while they resulted up to 15 fold more active than Flu against resistant strains of *Candida* species. All these three compounds possess the common 4-chloro-phenylpiperazino moiety

Table 2
Effect of **5e**,**f** and **6c** on the human lung adenocarcinoma epithelial cells (A549) growth.

	CC_{50} (μg mL^{-1})
5e	78.4 ± 2.2
5f	82.2 ± 5
6c	171.8 ± 14.2

CC_{50}: concentration (μg mL^{-1}) required to reduce cell viability by 50%. Data represent means ± standard deviation from two independent experiments, each performed in triplicate.

aligned to the A2 and HAL contour maps of the ligand-based model, that appears to be particularly important for the antifungal activity and to try to face the problem of drug resistance against *Candida* species. Experimental data show that (*S*)-**5f** is more active than its (*R*)-enantiomer and (*R*)-**6c** is more active than its (*S*)-enantiomer. Taking into account modelling results, it is not surprising since (*S*)-**5f** and (*R*)-**6c** perfectly align to the model, showing the same relative configuration (even if the absolute configuration is reversed). This because **6c** has a −NH− in plus with respect to **5f** that allows a movement leading to the alignment of (*R*)-**6c** N-[4-[4-(4-chlorophenyl)piperazin-1-yl]phenyl]carbamate moiety to (*S*)-**5f** 4-(4-chlorophenyl)piperazine-1-carboxilate group. Hence, from the modelling study we can speculate that to exert an antifungal activity, the relative configuration of compounds is of great

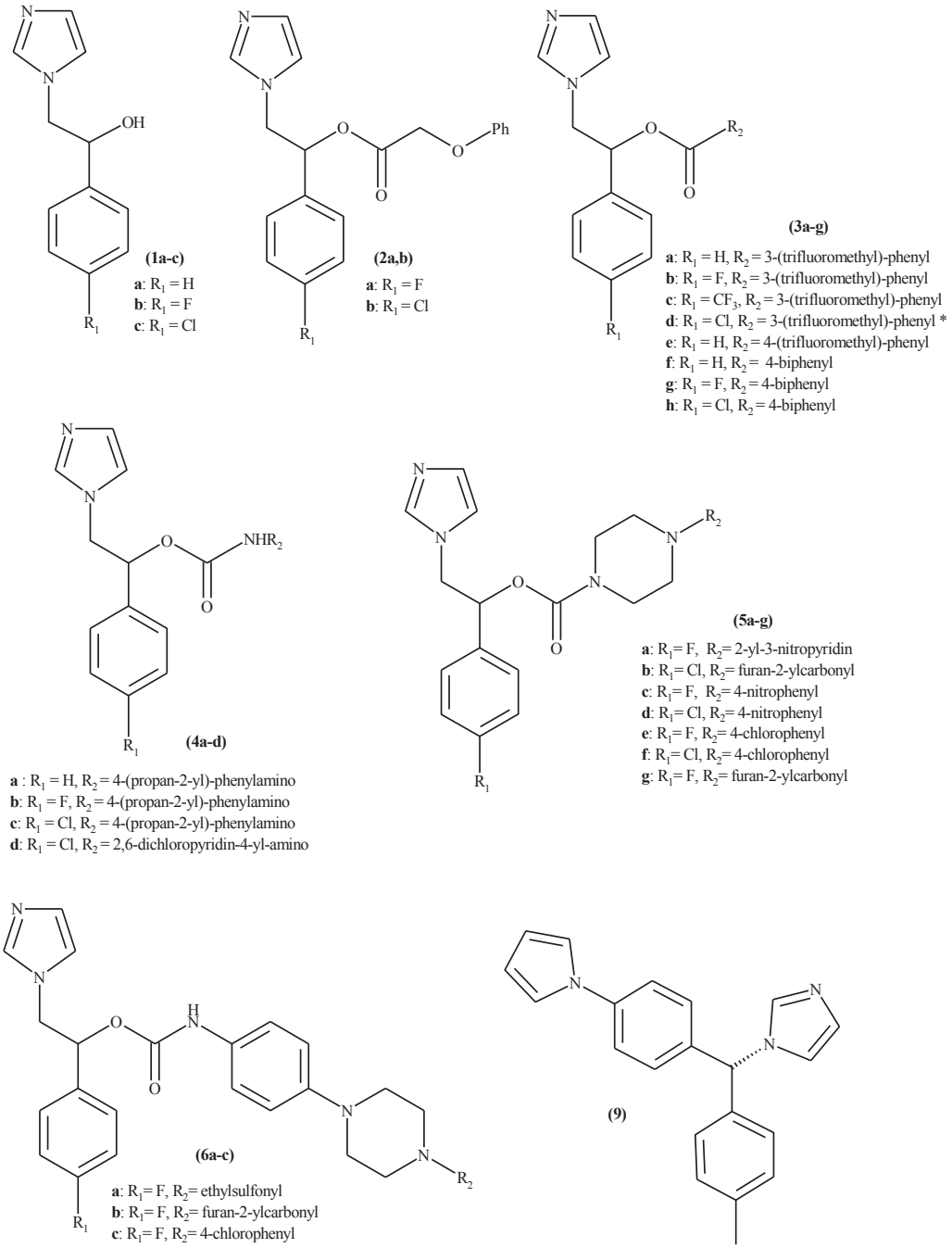

Chart 2. compounds described in this study.

importance, since only those in which the imidazole moiety aligns to the blue contour map and the 4-chloro-phenylpiperazino moiety aligns to the A2 and HAL contour maps of the ligand-based model show a high activity *in vitro*. The confirmation of the target of the synthesized azole-based compounds and their further optimization through synthetic strategies at the light of the information obtained by molecular modelling, will be the theme of the future work.

4. Experimental

4.1. Chemistry

All reagents and solvents were of high analytical grade and were purchased from Sigma–Aldrich (Milano, Italy). 2-(1H-imidazol-1-yl)-1-phenylethanol derivatives **1a**–**c**, **2a**,**b**, **3a**–**g**, **4a**–**c** were prepared according to the literature procedure [10]. The pure enantiomers of **1b**,**c** have been prepared as previously described [11] and used for the synthesis of the enantiomeric pure carbamates; analytical HPLC analysis of these final compounds were performed using the commercially available 250 mm × 4.6 mm I.D. Chiralcel OD column (Chiral Technologies Europe, Illkirch, France). HPLC grade ethanol was purchased from Aldrich (St. Louis, Missouri USA). The analytical HPLC apparatus consisted of a Perkin Elmer (Norwalk, CT, USA) 200 LC pump equipped with a Rheodyne (Cotati, CA, USA) injector, a 20 mL sample loop, an HPLC Dionex CC-100 oven (Sunnyvale, CA, USA) and a Jasco (Jasco, Tokyo, Japan) Model CD 2095 Plus UV/CD detector. All the enantiomeric final compounds showed an optical purity higher than 99.9% e.e.. Melting points were determined on Tottoli apparatus (Buchi) and are uncorrected. Infrared spectra were recorded on a Spectrum One ATR Perkin Elmer FT-IR spectrometer. ^{1}H NMR and ^{13}C NMR spectra were acquired on a Bruker AVANCE-400 spectrometer at 9.4 T, in $CDCl_3$, CD_3OD or DMSO-d_6 at 27 °C; chemical shift values are given in δ (ppm) relatively to TMS as internal reference. Coupling constants are given in Hz. Mass spectrometric experiments were carried out with a 2000 Q TRAP instrument (Applied Biosystems), a commercial hybrid triple-quadrupole linear ion-trap mass spectrometer (Q1q2QLIT), equipped with an ESI source and a syringe pump have been used. The examined compounds were previously dissolved in methanol (10^{-5} M) and aqueous HCl was added just before the injection. The molecular peaks (m/z) have been observed as $[M+H]^+$. Elemental analyses were obtained by a PE 2400 (Perkin–Elmer) analyzer and the analytical results were within ±0.4% of the theoretical values for all compounds.

4.2. Synthesis of carbamates **5a**–**f**, **6a**–**c**

4.2.1. General procedure to obtain nitrocompounds **7a**–**c**

1 mmol of 1-substituted piperazine was dissolved in 5 mL of CH_3CN, then 2.5 mmol of 1-fluoro-4-nitrobenzene were added. The mixture was refluxed for 2 h, then the solvent was removed and the crude residue was purified by silica gel column chromatography, using dichloromethane/methanol (9:1) as eluent.

*4.2.1.1. 1-(Ethylsulfonyl)-4-(4-nitrophenyl)piperazine (**7a**).* Yield 64%, as yellow solid. ^{1}H NMR ($CDCl_3$): δ 8.11 (d, 2H, J = 9.0 Hz), 6.86 (d, 2H, J = 9.0 Hz), 3.48 (m, 8H), 3.00 (q, 2H, J = 7.3 Hz), 1.40 (t, 3H, J = 7.3 Hz).

*4.2.1.2. Furan-2-yl[4-(4-nitrophenyl)piperazin-1-yl]methanone (**7b**).* Yield 53%, as yellow solid. ^{1}H NMR ($CDCl_3$): δ 8.17 (d, 2H, J = 9.3 Hz), 7.53 (s, 1H), 7.11 (d, 1H, J = 3.4 Hz), 6.86 (d, 2H, J = 9.3 Hz), 6.53 (m, 1H), 4.03 (m, 4H), 3.55 (m, 4H).

*4.2.1.3. 1-(4-Chlorophenyl)-4-(4-nitrophenyl)piperazine (**7c**).* Yield 43%, as yellow solid. ^{1}H NMR (DMSO-d_6): δ 8.08 (d, 2H, J = 9.3), 7.26 (d, 2H, J = 8.3), 7.08 (d, 2H, J = 8.8), 7.00 (d, 2H, J = 8.3), 3.63 (m, 4H); 4H piperazine overlap.

4.2.2. Synthesis of 1-(3-nitro-2-pyridyl)piperazine (**7d**)

3 mmol of piperazine dihydrochloride hydrate was added of 10 mL of CH_3CN, TEA (6 mmol) and 2-chloro-3-nitropyridine (1 mmol). After 2 h, at reflux, the mixture was evaporated under reduced pressure and the residue was treated with H_2O (5 mL) and ethylacetate (5 mL). The aqueous phase was separated and extracted twice with ethylacetate (2 × 5 mL). The combined organic phases were dried on Na_2SO_4, filtered and evaporated under reduced pressure. The crude residue was purified by silica gel column chromatography, using dichloromethane/methanol (9:1) as eluent. Yield 62%, as yellow solid. ^{1}H NMR (DMSO-d_6): 8.44 (dd, 1H, J = 4.5 Hz, J = 1.6 Hz), 8.29 (dd, 1H, J = 8.1 Hz, J = 1.6 Hz), 6.94 (dd, 1H, J = 8.1 Hz, J = 4.5 Hz), 3.56 (m, 4H), 2.80 (m, 4H).

4.2.3. General procedure for the preparation of amines **8a**–**c**

1 mmol of the nitrocompound (**7a**–**c**) was suspended in 90 mL of MeOH and then reduced by hydrogenation at 50 psi in the presence of 10% Pd/C (10 mg) as catalyst, for 4 h at room temperature. The catalyst was removed by filtration, the solution was evaporated under reduce pressure to give **8a**–**c** immediately used for the subsequent reaction.

4.2.4. General procedure for the synthesis of (1H-imidazol-1yl)-ethyl carbamates **5a**–**f**, **6a**–**c**

2-(1H-imidazol-1-yl)-1-phenylethanol (1 mmol) was suspended in 5 mL of anhydrous CH_3CN, then triphosgene (0.5 mmol) was added. After 12 h at r.t. the reaction mixture was treated with Et_2O obtaining a white precipitate, subsequently the solvent was removed and the precipitate was suspended in anhydrous CH_3CN and added with TEA (2.0 mmol) and 0.8 mmol of the selected amine. After 12 h at r.t., the solvent was removed under reduced pressure and the residue was treated with CH_2Cl_2 and extracted with saturated aqueous Na_2CO_3. The organic layer was dried over Na_2SO_4 and evaporated under vacuum to give a crude residue which was purified by silica gel column chromatography using CH_2Cl_2/MeOH (8:2) as eluent.

*4.2.4.1. [1-(4-Fluorophenyl)-2-imidazol-1-yl-ethyl]4-(2-nitro-3-pyridyl)piperazine-1-carboxylate (**5a**).* Yield 65%, as yellow solid. Mp: 143–5. ^{1}H NMR (CD_3OD): δ 8.40 (d, 1H, J = 4.4 Hz), 8.25 (d, 1H, J = 8.0 Hz), 7.81 (s, 1H), 7.40 (m, 2H), 7.23 (s, 1H), 7.14 (m, 2H), 7.07 (s, 1H), 6.95 (dd, 1H, J = 4.4 Hz, J = 8.0 Hz), 6.01 (m, 1H), 4.50 (m, 2H), 3.74–3.43 (m, 8H). ^{13}C NMR (CD_3OD): δ 162.8 (J = 243.0 Hz), 154.0, 152.6, 151.5, 137.7, 135.3, 133.9, 133.4, 128.1 (J = 8.0 Hz), 127.5, 120.0, 115.1 (J = 22.0 Hz), 114.3, 75.3, 51.1, 43.4, 43.1. IR: υ 1686 cm^{-1}. MS, m/z: 441.00 $[M+H]^+$.

*4.2.4.2. [1-(4-Chlorophenyl)-2-imidazol-1-yl-ethyl]4-(furan-2-carbonyl)piperazine-1-carboxylate (**5b**).* Yield 60%, as waxy solid. ^{1}H NMR ($CDCl_3$): δ 7.28–7.13 (m, 4H), 7.03 (m, 3H), 6.83 (d, 2H, J = 8.3 Hz), 6.75 (s, 1H), 5.93 (t, 1H, J = 6.0 Hz), 4.29 (m, 2H), 3.63 (m, 4H), 3.10 (m, 4H). ^{13}C NMR (DMSO-d_6): δ 158.9, 153.3, 147.2, 145.4, 136.7, 136.4, 133.6, 129.1, 128.6, 122.9, 121.4, 116.4, 111.8, 74.3, 52.6, 43.9, 43.9 IR: υ 1701-1622 cm^{-1}. MS, m/z: 428. 98 $[M+H]^+$.

*4.2.4.3. [1-(4-Fluorophenyl)-2-imidazol-1-yl-ethyl] 4-(4-nitrophenyl)piperazine-1-carboxylate (**5c**).* Yield 70%, as a yellow solid. Mp: 168–9. ^{1}H NMR ($CDCl_3$): δ 8.13 (d, 2H, J = 8.9 Hz), 7.84 (s, 1H), 7.22 (m, 2H), 7.07 (m, 3H), 6.81 (m, 3H), 5.98 (t, 1H, J = 5.2 Hz), 4.39 (m, 2H), 3.67 (m, 4H), 3.42 (m, 4H). ^{13}C NMR ($CDCl_3$) δ: 162.9

(J = 247 Hz), 154.4, 153.5, 139.3, 137.5, 132.4 (J = 3 Hz), 128.2, 128.0 (J = 8 Hz), 125.9, 119.8, 116.1 (J = 22 Hz), 113.2, 77.2, 74.9, 52.1, 46.8. IR: υ 1704 cm^{-1}. MS, m/z: 439.93 $[M+H]^+$.

*4.2.4.4. [1-(4-Chlorophenyl)-2-imidazol-1-yl-ethyl] 4-(4-nitrophenyl)piperazine-1-carboxylate (**5d**).* Yield 80%, as a yellow solid. Mp: 188–190. ^1H NMR ($CDCl_3$): δ 8.14 (d, 2H, J = 9.3 Hz), 7.45 (s, 1H), 7.34 (m, 2H), 7.14 (d, 2H, J = 10.5 Hz),7.04 (s, 1H) 6.81 (m, 3H), 5,94 (t, 1H, J = 5.5 Hz), 4.33 (m, 2H), 3.67 (m, 4H), 3.42 (m, 4H). ^{13}C NMR ($CDCl_3$) δ: 154.4, 153.5, 139.2, 137.6, 135.2, 135.0, 129.2, 129.1, 127.5, 125.9, 119.7, 113.1, 75.0, 51.7, 46.8, 43.3. IR: υ 1704 cm^{-1}. MS, m/z: 455.97 $[M+H]^+$.

*4.2.4.5. [1-(4-Fluorophenyl)-2-imidazol-1-yl-ethyl] 4-(4-chlorophenyl)piperazine-1-carboxylate (**5e**).* Yield 92%, as a waxy solid. ^1H NMR (DMSO-d_6): δ 7.56 (s, 1H), 7.38 (dd, 2H, J = 5.5 Hz, J = 7.8 Hz), 7.24–7.13 (m, 5H), 6.95 (d, 2H, J = 8.9 Hz), 6.84 (s, 1H), 5.83 (m, 1H), 4.36 (m, 2H), 3.37 (m, 4H), 3.04 (m, 4H). ^{13}C NMR (DMSO-*d6*) δ: 161.8 (J = 243 Hz), 153.2, 149.6, 137.9, 134.2 (J = 2 Hz), 128.7, 128.4 (J = 9 Hz), 128.1, 122.9, 120.0, 117.4, 115.3 (J = 22 Hz), 74.7, 50.6, 48.1, 43.2. IR: υ 1703 cm^{-1}. MS, m/z: 428.89 $[M+H]^+$.

*4.2.4.6. 1-(4-Chlorophenyl)-2-imidazol-1-yl-ethyl] 4-(4-chlorophenyl)piperazine-1-carboxylate (**5f**).* Yield 88%, as a white solid. Mp: 113–6. ^1H NMR (DMSO-d_6): δ 7.53 (s, 1H), 7.45 (d, 2H, J = 8.3 Hz), 7.37 (d, 2H, J = 8.3 Hz), 7.25 (d, 2H, J = 8.9 Hz), 7.13 (s, 1H), 6.97 (d, 2H, J = 8.9 Hz), 6.84 (s, 1H), 5.86 (m, 1H), 4.38 (m, 2H), 3.65 (m, 4H), 3.09 (m, 4H). ^{13}C NMR (DMSO-d_6): δ 153.8, 149.9, 137.8, 136.2, 134.1, 128.7, 128.6, 127.7, 127.4, 124.7, 120.1, 117.7, 75.1, 51.1, 48.9, 43.4 IR: υ 1702 cm^{-1}. MS, m/z: 444.87 $[M+H]^+$.

*4.2.4.7. [1-(4-Fluorophenyl)-2-imidazol-1-yl-ethyl]4-(furan-2-carbonyl)piperazine-1-carboxylate (**5g**).* Yield 78%, as a waxy solid. ^1H NMR (CD_3OD): δ 7.71 (s, 1H), 7.41–7.38 (m, 2H), 7.14–7.08 (m, 5H), 6.97 (s, 1H), 6.61 (s, 1H), 5.99 (t, 1H, J = 6.0 Hz), 4.49–4.42 (m, 2H), 3.90–3.40 (m, 8H). ^{13}C (CD_3OD): δ 164.2 (J = 244 Hz), 161.2, 155.3, 148.2, 146.1, 139.2, 134.7 (J = 3 Hz), 129.6 (J = 8 Hz), 129.0, 121.5, 118.0, 116.5 (J = 22 Hz), 112.5, 76.8, 73.5, 55.3, 52.5. IR: υ 1699, 1621 cm^{-1}. MS, m/z: 412.99 $[M+H]^+$.

*4.2.4.8. [1-(4-Fluorophenyl)-2-imidazol-1-yl-ethyl]N-[4-(4-ethylsulfonylpiperazin-1-yl)phenyl]carbamate (**6a**).* Yield 37%, as a white solid. Mp: 113–5. ^1H NMR (DMSO-d_6): δ 9.64 (s broad, 1H), 7.55 (s, 1H), 7.40 (m, 2H), 7.28–7.15 (m, 5H), 6.90 (d, 2H, J = 8.9 Hz), 6.85 (s, 1H), 5.94 (m, 1H), 4.41 (m, 2H), 3.30 (m, 4H, partially obscured by HDO signal, it appears after D_2O exchange), 3.09 (m, 6H), 1.23 (t, 3H, J = 7.5 Hz). ^{13}C NMR ($CDCl_3$): δ 162.8 (J = 246.0 Hz), 152.5, 147.2, 138.1, 132.8, 131.4, 128.2, 127.9 (J = 8.0 Hz), 120.2, 120.0, 117.7, 115.8 (J = 22.0 Hz), 73.9, 52.1, 50.2, 45.8, 44.0, 7.8. IR: υ 1707 cm^{-1}. MS, m/z: 501.93 $[M+H]^+$.

*4.2.4.9. [1-(4-Fluorophenyl)-2-imidazol-1-yl-ethyl] N-[4-[4-(furan-2-carbonyl)piperazin-1-yl]phenyl]carbamate (**6b**).* Yield 71%, as a white solid. Mp: 89–91. ^1H NMR (DMSO-d_6): δ 9.62 (s broad, 1H), 7.86 (s, 1H), 7.54 (s, 1H), 7.39 (m, 2H), 7.27–7.15 (m, 5H), 7.02 (d, 1H, J = 2.9 Hz), 6.90, (d, 2H, J = 8.4 Hz), 6.84 (s, 1H), 6.64 (s, 1H), 5.94 (m, 1H), 4.41 (m, 2H), 3.80 (m, 4H), 3.19 (m, 4H). ^{13}C NMR ($CDCl_3$): δ 162.7 (J = 247 Hz), 159.1, 152.5, 147.9, 143.8, 138.1, 132.7 (J = 3 Hz), 131.0, 127.9 (J = 8 Hz), 120.4, 120.3, 120.0, 117.4, 117.3, 116.7, 115.8 (J = 21 Hz), 111.4, 73.9, 72.3, 52.1, 50.2. IR: υ 1714, 1602 cm^{-1}. MS, m/z: 504.00 $[M+H]^+$.

*4.2.4.10. [1-(4-Fluorophenyl)-2-imidazol-1-yl-ethyl] N-[4-[4-(4-chlorophenyl)piperazin-1-yl]phenyl]carbamate (**6c**).* Yield 74%, as a white solid. Mp: 209–211. ^1H NMR (DMSO-d_6): δ 9.62 (s broad, 1H), 7.55 (s, 1H), 7.40 (m, 2H), 7.29–7.15 (m, 7H), 7.01 (d, 2H, J = 8.8 Hz), 6.93 (d, 2H, 8.2 Hz), 6.85 (s, 1H), 5.94 (m, 1H), 4.41 (m, 2H), 3.26 (m, 4H, partially obscured by HDO signal, it appears after D_2O exchange), 3.18 (m, 4H). ^{13}C NMR (CD_3OD): δ 162.7 (J = 243 Hz), 153.2, 151.4, 150.1, 133.5 (J = 2.5 Hz), 128.7, 128.5, 128.0 (J = 8 Hz), 127.4, 124.4, 120.1, 119.9; 117.4, 116.9, 116.3, 115.0 (J = 21 Hz), 74.2, 51.3, 49.8, 49.4. IR: υ 1721 cm^{-1}. MS, m/z: 520.03 $[M+H]^+$.

4.3. Organisms

For the antifungal evaluation, strains obtained from the American Type Culture Collection (ATCC, Rockville, MD, USA), the German Collection of Microorganisms (DSMZ, Braunschweig, Germany) and the Pharmaceutical Microbiology Culture Collection (PMC, Department of Public Health and Infectious Diseases, "Sapienza" University, Rome, Italy) were tested. The strains were:

C. albicans (ATCC24433, ATCC10231, ATCC76615, ATCC10261, ATCC90028,

ATCC20891, 3153, PMC1011, PMC1040R, PMC1041R, PMC1042R), *Candida krusei* (DSM6128 and PMC0613), *Candida tropicalis* (DSM11953 and PMC0910), *Candida parapsilosis* (ATCC22019, DSM11224), *Candida glabrata* (PMC0805, PMC0807, PMC0850R, PMC0851R, PMC0852R, PMC0853R), *C. neoformans* (DSM11959, PMC2136, PMC2123, PMC2115, PMC2103, PMC2107, PMC2102, and PMC2111), *Trichophyton mentagrophytes* (DSM 4870, PMC6515, PMC6531, PMC6503, PMC6509, PMC6552), *Microsporum gypseum* (DSM3824, PMC7331 and PMC7303). All of the strains were stored and grown in accordance with the procedures of the Clinical and Laboratory Standards Institute (CLSI) [15,16].

4.4. Antifungal susceptibility assays

In vitro antifungal susceptibility was evaluated for all compounds, using the CLSI broth microdilution methods [15,16]. Fluconazole and Amphotericin B were used as reference drug. The final concentration ranged from 0.125 to 64 μg mL^{-1} for all compounds. The compounds were dissolved previously in dimethyl sulfoxide at concentrations 100 times higher than the highest desired test concentration and successively diluted in test medium in accordance with the procedures of the CLSI [17].

Microdilution trays containing 100 μL of serial two-fold dilutions of compound in RPMI 1640 medium (Sigma Aldrich, St. Louis, Missouri, U.S.A) were inoculated with an organism suspension adjusted to attain a final inoculum concentration of 1.0×10^3 and 1.5×10^3 cells mL^{-1} for yeasts and 0.4×10^4 and 5×10^4 CFU mL^{-1} for dermatophytes. The panels were incubated at 35 °C and observed for the presence of growth at 48 h (*Candida* spp.) and 72 h (*C. neoformans* and dermatophytes).

The MIC defined as, for yeasts, the lowest concentration that showed ≥50% growth inhibition compared with the growth control and, for dermatophytes, the lowest concentration that showed ≥80% growth inhibition compared with the growth control was evaluated for all compounds. The results were expressed as the median of the MIC values of five replicates, and the geometric mean (GM) values.

4.5. Cell viability assay

The cytotoxicity of tested new compounds was evaluated on human lung adenocarcinoma epithelial cell line (A549) obtained from American Type Culture Collection (ATCC CCL-185, Rockville, MD, USA) by using a 3-(4,5-dimethylthiazol-2-yl)-2,5-diphenyltetrazolium bromide (MTT) reduction assay. The cells (2×10^4 cells/well) were seeded into 96-well plates containing 100 μl of supplemented RPMI 1640 (Invitrogen, San Diego, CA, USA) without phenol red, supplemented with 10% foetal bovine

serum (Invitrogen, San Diego, CA, USA), L-glutamine (0.3 mg mL^{-1}), penicillin (100 U mL^{-1}), and streptomycin (100 μg mL^{-1}) (EuroClone, Celbio, Milan, Italy), and they were cultured at 37 °C in 5% CO_2. The cells were exposed to the indicated compounds (dissolved in dimethyl sulfoxide, DMSO) at the final concentration ranging from 16 to 256 μg mL^{-1}. Each concentration and control was assayed in three replicates with at least five concentrations. The cells were cultured at 37 °C and 5% CO_2 for 48 h. MTT solution (Sigma–Aldrich, St. Louis, Missouri, U.S.A.) was added to each well in an amount equal to 10% of the culture volume, and the plates were incubated for 3–4 h at 37 °C in 5% CO_2. MTT solvent (Sigma–Aldrich, St. Louis, Missouri, U.S.A.) was successively added to dissolve the intracellular crystal. The plates were then incubated at 37 °C in 5% CO_2, and the optical density of each well was measured spectrophotometrically at 570 nm. The cytotoxicity of the compounds was calculated as percentage reduction in viable cells with respect to the control culture (cells treated with DMSO only). The 50% cytotoxic concentration (CC_{50}) was evaluated as the drug concentration required to reduce human cell viability by 50% compared to the drug-free control.

4.6. Design and pretreatment of the synthesized azole-based compounds and generation of a ligand-based model

The synthesized azole-based compounds and the reference antifungal drug Fluconazole were designed by means of Maestro9.2 and pretreated with LigPrep [18,19]. The ionization state of all compounds was checked at pH 7 ± 1 using Epik [20]. −R and −S enantiomers were generated by means of FLAP at default settings [21]. The sampling of the conformational space was performed according to a stochastic search using the MM3 force field. The alignment of all the stereoisomers and their conformers were performed by means of FLAP at default settings according to the bond type similarity. For the compounds not experimentally separated, the enantiomers to be considered for the generation of the ligand-based model were selected automatically by the software. For the compounds experimentally separated, both (*R*)- and (*S*)-enantiomers where introduced in the alignment procedure. Compounds were automatically cat into a training set and a test set according to GRID MIFs in a ratio of 1:1. The computation of the ligand-based model was performed with an accuracy of 150% applying the dissimilarity penalty and was validated by means of the leave-one-out method. Potential contour maps were identified by default GRID probes.

Acknowledgements

This work was supported by the Project PON 01_01802. We are indebted to Molecular Discovery for access to the FLAP code.

Appendix A. Supplementary data

Supplementary data related to this article can be found at http://dx.doi.org/10.1016/j.ejmech.2014.07.001. These data include MOL files and InChiKeys of the most important compounds described in this article.

References

[1] G.D. Brown, D.W. Denning, S.M. Levitz, Tackling human fungal infections, Science 336 (6082) (2012) 647.
[2] M.K. Kathiravan, A.B. Salake, A.S. Chothe, P.B. Dudhe, R.P. Watode, M.S. Mukta, S. Gadhwe, The biology and chemistry of antifungal agents: a review, Bioorg. Med. Chem. 20 (19) (2012) 5678–5698.
[3] M.I. Attia, A.S. Zaharia, M.S. Almutairi, S.W. Ghoneim, In vitro anti-Candida activity of certain new 3-(1H-imidazol-1-yl)propan-1-one oxime esters, Molecules 18 (10) (2013) 12208–12221.
[4] S.C. Chen, E.G. Playford, T.C. Sorrell, Antifungal therapy in invasive fungal infections, Curr. Opin. Pharmacol. 10 (5) (2010) 522–530.
[5] Y. Zou, S. Yu, R. Li, Q. Zhao, X. Li, M. Wu, T. Huang, X. Chai, H. Hu, Q. Wu, Synthesis, antifungal activities and molecular docking studies of novel 2-(2,4-difluorophenyl)-2-hydroxy-3-(1H-1,2,4-triazol-1-yl)propyl dithiocarbamates, Eur. J. Med. Chem. 74 (2014) 366–374.
[6] J. Loeffler, D.A. Stevens, Antifungal drug resistance, Clin. Infect. Dis. 36 (Suppl. 1) (2003) S31–S41.
[7] L. Li, H. Ding, B. Wang, S. Yu, Y. Zou, X. Chai, Q. Wu, Synthesis and evaluation of novel azoles as potent antifungal agents, Bioorg. Med. Chem. Lett. 24 (1) (2014) 192–194.
[8] E.K. Spanakis, G. Aperis, E. Mylonakis, New agents for the treatment of fungal infections: clinical efficacy and gaps in coverage, Clin. Infect. Dis. 43 (8) (2006) 1060–1068.
[9] B.E. Elewski, Onychomycosis. Treatment, quality of life, and economic issues, Am. J. Clin. Dermatol. 1 (1) (2000) 19–26.
[10] D. De Vita, L. Scipione, S. Tortorella, P. Mellini, B. Di Renzo, G. Simonetti, F.D. D'Auria, S. Panella, R. Cirilli, R. Di Santo, A.T. Palamara, Synthesis and antifungal activity of a new series of 2-(1H-imidazol-1-yl)-1-phenylethanol derivatives, Eur. J. Med. Chem. 49 (2012) 334–342.
[11] L. Friggeri, L. Scipione, R. Costi, M. Kaiser, F. Moraca, C. Zamperini, B. Botta, R. Di Santo, D. De Vita, R. Brun, S. Tortorella, New promising compounds with in vitro nanomolar activity against *Trypanosoma cruzi*, ACS Med. Chem. Lett. 4 (2013) 538–541.
[12] A. Tafi, R. Costi, M. Botta, R. Di Santo, F. Corelli, S. Massa, A. Ciacci, F. Manetti, M. Artico, Antifungal agents. 10. New derivatives of 1-[(aryl)[4-aryl-1H-pyrrol-3-yl]methyl]-1H-imidazole, synthesis, anti-candida activity, and quantitative structure–analysis relationship studies, J. Med. Chem. 45 (13) (2002) 2720–2732.
[13] B. Rupp, S. Raub, C. Marian, A.D. Holtje, Molecular design of two sterol 14alpha-demethylase homology models and their interactions with the azole antifungals ketoconazole and bifonazole, J. Comput. Aided Mol. Des. 19 (3) (2005) 149–163.
[14] R. Di Santo, A. Tafi, R. Costi, M. Botta, M. Artico, F. Corelli, M. Forte, F. Caporuscio, L. Angiolella, A.T. Palamara, Antifungal agents. 11. N-Substituted derivatives of 1-[(Aryl)(4-aryl-1H-pyrrol-3-yl)methyl]-1H-imidazole: synthesis, anti-candida activity, and QSAR studies, J. Med. Chem. 48 (16) (2005) 5140–5153.
[15] Clinical and Laboratory Standards Institute, Reference Method for Broth Dilution Antifungal Susceptibility Testing of Yeasts, 2008. Approved Standard M27 A3, Wayne, PA.
[16] Clinical and Laboratory Standards Institute, Reference Method for Broth Dilution Antifungal Susceptibility Testing of Filamentous Fungi, 2008. Approved Standard M38 A2, Wayne, PA.
[17] Clinical and Laboratory Standards Institute, Reference Method for Broth Dilution Antifungal Susceptibility Testing of Yeasts, 2008. Informational Supplement M27S3, Wayne, PA.
[18] Maestro, Version 9.2, Schrödinger, LCC, New York, NY, 2011.
[19] LigPrep, Version 2.5, Schrödinger, LCC, New York, NY, 2011.
[20] Epik, Version 2.2, Schrödinger, LCC, New York, NY, 2011.
[21] M. Baroni, G. Cruciani, S. Sciabola, F. Perruccio, J.S. Mason, A common reference framework for analyzing/comparing proteins and ligands. Fingerprints for ligands and proteins (FLAP): theory and application, J. Chem. Inf. Model. 47 (2) (2007) 279–294.